


# Aquatic export of young dissolved and gaseous carbon from a pristine boreal fen: Implications for peat carbon stock stability

Audrey Campeau<sup>1</sup>  | Kevin H. Bishop<sup>2</sup> | Michael F. Billett<sup>3</sup> | Mark H. Garnett<sup>4</sup> | Hjalmar Laudon<sup>5</sup> | Jason A. Leach<sup>6</sup> | Mats B. Nilsson<sup>5</sup> | Mats G. Öquist<sup>5</sup> | Marcus B. Wallin<sup>1</sup>

<sup>1</sup>Department of Earth Sciences, Air water and Landscape, Uppsala University, Uppsala, Sweden

<sup>2</sup>Department of Aquatic Sciences and Assessment, Swedish University of Agricultural Sciences, Uppsala, Sweden

<sup>3</sup>Biological and Environmental Sciences, Faculty of Natural Sciences, University of Stirling, Stirling, UK

<sup>4</sup>NERC Radiocarbon Facility, Scottish Enterprise Technology Park, East Kilbride, Glasgow, UK

<sup>5</sup>Department of Forest Ecology and Management, Swedish University of Agricultural Sciences, Umeå, Sweden

<sup>6</sup>Department of Geography, Simon Fraser University, Burnaby, BC, Canada

## Correspondence

Audrey Campeau, Department of Earth Sciences, Uppsala University, Uppsala, Sweden.

Email: [audrey.campeau@geo.uu.se](mailto:audrey.campeau@geo.uu.se)

## Funding information

Swedish Research Council, Grant/Award Number: 2012–3919; Uppsala University; Knut and Alice Wallenberg foundation; Natural Environment Research Council, Grant/Award Number: NRCF010001

## Abstract

The stability of northern peatland's carbon (C) store under changing climate is of major concern for the global C cycle. The aquatic export of C from boreal peatlands is recognized as both a critical pathway for the remobilization of peat C stocks as well as a major component of the net ecosystem C balance (NECB). Here, we present a full year characterization of radiocarbon content (<sup>14</sup>C) of dissolved organic carbon (DOC), carbon dioxide (CO<sub>2</sub>), and methane (CH<sub>4</sub>) exported from a boreal peatland catchment coupled with <sup>14</sup>C characterization of the catchment's peat profile of the same C species. The age of aquatic C in runoff varied little throughout the year and appeared to be sustained by recently fixed C from the atmosphere (<60 years), despite stream DOC, CO<sub>2</sub>, and CH<sub>4</sub> primarily being sourced from deep peat horizons (2–4 m) near the mire's outlet. In fact, the <sup>14</sup>C content of DOC, CO<sub>2</sub>, and CH<sub>4</sub> across the entire peat profile was considerably enriched with postbomb C compared with the solid peat material. Overall, our results demonstrate little to no mobilization of ancient C stocks from this boreal peatland and a relatively large resilience of the source of aquatic C export to forecasted hydroclimatic changes.

## KEYWORDS

aquatic C export, carbon dioxide, dissolved organic carbon, methane, northern peatlands, radiocarbon dating

## 1 | INTRODUCTION

Northern peatlands have a central role in the global carbon (C) cycle, being the repository of a third of the global soil organic matter (~450 Pg; Gorham, 1991) and persistent sinks of contemporary atmospheric CO<sub>2</sub> (Lund et al., 2010; Nilsson et al., 2008; Roulet et al., 2007). The stability of northern peatland's C stocks and their role in the C cycle under changing climate and increasing anthropogenic pressure is of major concern (Crowther et al., 2016; Wilson et al.,

2016). The aquatic export of C represents a major pathway for the mobilization of ancient peat C stocks, as well as being a critical component of the net ecosystem C balance (NECB; Billett, Garnett, & Dinsmore, 2015; Dinsmore et al., 2010; Nilsson et al., 2008). It comprises organic C (TOC) and dissolved inorganic C (DIC), along with gaseous forms; mainly carbon dioxide (CO<sub>2</sub>), and methane (CH<sub>4</sub>), all of which can arise from the breakdown of either "old" peat material or more recently fixed carbon from the atmosphere (Billett et al., 2015; Leach, Larsson, Wallin, Nilsson, & Laudon, 2016; Wallin et al., 2013).

This is an open access article under the terms of the Creative Commons Attribution License, which permits use, distribution and reproduction in any medium, provided the original work is properly cited.

© 2017 The Authors *Global Change Biology* Published by John Wiley & Sons Ltd

The distinction between these two sources is relevant to the stability of a peatland's C stock, as well as providing information about the links between different flux components in the NECB. Changes in climate and hydrology are known to exert a strong control on the magnitude of each component in a peatland's NECB, including the net ecosystem exchange (NEE) (Nijp et al., 2015; Peichl et al., 2014), CH<sub>4</sub> emissions (Bellisario, Bubier, Moore, & Chanton, 1999; Wilson et al., 2016), C accumulation (Frolking et al., 2001), and aquatic C export (Leach et al., 2016). Whether these drivers influence the source dynamics of a peatland's aquatic C export is to a large extent unknown (Wilson et al., 2016). Identifying the source of aquatic C export will help predict NECB response to environmental changes.

The radiocarbon content (<sup>14</sup>C) and stable isotope composition ( $\delta^{13}\text{C}$ ) of C can help elucidate the sources of C. The reported <sup>14</sup>C content of aquatic C export from peatlands is notably variable across spatial and temporal scales, as well as between C species (Butman, Wilson, Barnes, Xenopoulos, & Raymond, 2014; Evans et al., 2014; Garnett, Dinsmore, & Billett, 2012), thus drawing further attention to the complex mixture of sources contributing to aquatic C export in the NECB (Billett et al., 2015). The currently available data suggest that the age of stream DOC, CO<sub>2</sub>, or CH<sub>4</sub> exported from peat-dominated catchments can range from modern to >1,000 years (Billett et al., 2015; Evans et al., 2014; Garnett et al., 2012). Only a few studies have repeated <sup>14</sup>C characterization in streams over time (Garnett et al., 2012; Schiff et al., 1997; Tipping, Billett, Bryant, Buckingham, & Thacker, 2010). These studies suggest that stream C age can change significantly over a complete annual cycle, with changes in <sup>14</sup>C content corresponding to as much as 500 years when expressed in conventional <sup>14</sup>C years. Major discrepancies in <sup>14</sup>C content between DOC, CO<sub>2</sub>, and CH<sub>4</sub> within the same stream have also been observed, with differences of up to 1,000 years between the different C species (Billett, Garnett, & Harvey, 2007; Garnett, Hardie, Murray, & Billett, 2013; Leith, Garnett, Dinsmore, Billett, & Heal, 2014). Together, these results emphasize that aquatic C export from peatlands can arise from a variety of C sources and transport mechanisms. Hence, individual catchment studies are still needed to develop a more generalized understanding of the role of peatlands in the global C cycle.

Despite the highly variable <sup>14</sup>C content of C export in streams, a few reoccurring patterns can be discerned in the existing literature (Marwick et al., 2015). On many occasions, stream DIC is found to be older than DOC. Such differences are typically attributed to a partial sourcing of the DIC from carbonate dissolution (Billett et al., 2007; Mayorga et al., 2005; Vihermaa, Waldron, Garnett, & Newton, 2014). But, aged DIC has also been reported in peatland streams where such minerals do not seem to contribute to DIC, suggesting instead a partial sourcing from mineralization of older peat (Garnett et al., 2012) or preferential mineralization of <sup>14</sup>C-depleted fractions of the OC pool (Mccallister & Del Giorgio, 2012). The occurrence of <sup>14</sup>C-depleted DOC, on the other hand, has been linked to both anthropogenic disturbance and increasing sediment load to inland waters (Butman et al., 2014; Marwick et al., 2015; Moore et al., 2013). Older CH<sub>4</sub> compared with CO<sub>2</sub> has also been reported in several peatland streams and attributed to ebullitive transport of CH<sub>4</sub>

from deep peat horizons or geological sources (Garnett et al., 2013; Leith et al., 2014). Several studies have also reported an increase in postbomb <sup>14</sup>C content with increasing stream discharge, suggesting that high-flow events tend to mobilize younger material, typically associated with more superficial hydrological flowpaths (Billett et al., 2012; Dyson et al., 2011; Garnett et al., 2012). In northern high latitudes, stream discharge can vary by several orders of magnitude over the course of a full year cycle, with a majority of the annual runoff generated during the spring freshet, contributing to more than half of the annual aquatic C export (Ågren, Berggren, Laudon, & Jansson, 2008; Dyson et al., 2011; Leach et al., 2016).

In this study, we characterized the <sup>14</sup>C content of aquatic DOC, CO<sub>2</sub>, and CH<sub>4</sub> exported from a boreal peatland over a complete hydrological year with the aim of determining their sources and major controls. Our case study was the Degerö Stormyr, an extensively studied pristine nutrient-poor fen in northern Sweden, where organic C has accumulated for >8,000 years (Larsson, Segerström, Laudon, & Nilsson, 2016; Leach et al., 2016; Nilsson et al., 2008; Peichl et al., 2014; Figure 1). A previous study on aquatic C export at Degerö suggested that a significant proportion of the runoff could be generated from deep peat horizons (Leach et al., 2016). Based on these combined findings, we hypothesized that aquatic C export will be comprised of a major <sup>14</sup>C-depleted component due to partial sourcing from breakdown of ancient peat C located in deep soil horizons. To test this hypothesis, we coupled our analysis of aquatic <sup>14</sup>C export with a full peat depth profile characterization of the <sup>14</sup>C content of the same three dissolved C species and previously published <sup>14</sup>C characterization of the solid peat material (Larsson et al., 2016; Nilsson, Klarqvist, Bohlin, & Possnert, 2001). This allowed us to identify the sources and main drivers of aquatic C export, information that is critical to determining the stability of the peatland C stock and its resilience to changes in climate and hydrology.

## 2 | MATERIALS AND METHODS

### 2.1 | Study site and instrumentation

The study was conducted within the Degerö Stormyr mire complex which is located ca 60 km north-west of Umeå, northern Sweden. The mire complex is located on a topographic high point (~270 m.a.s.l.; 64°11'N, 19°33'E) and has a total surface area of 6.5 km<sup>2</sup>, with a 55 m elevation gradient (Leach et al., 2016). Degerö Stormyr consists of a mosaic of interconnected mires divided by islets and ridges of glacial till and is classified as an oligotrophic fen. The underlying bedrock is composed predominantly of base-poor Svecofennian metasediments/metagraywacke and includes no known carbonate containing minerals. The water table position is typically within 20 cm of the peat surface during the growing season. The climate at the site is cold temperate humid with a persistent snow cover during November to April. The maximum thickness of the snow pack is usually around 60 cm. The depth of the winter soil frost typically ranges from 10 to 30 cm (Granberg, Ottosson-Löfvenius, Grip, Sundh, & Nilsson, 2001). The 30 year (1981–2010) mean annual precipitation

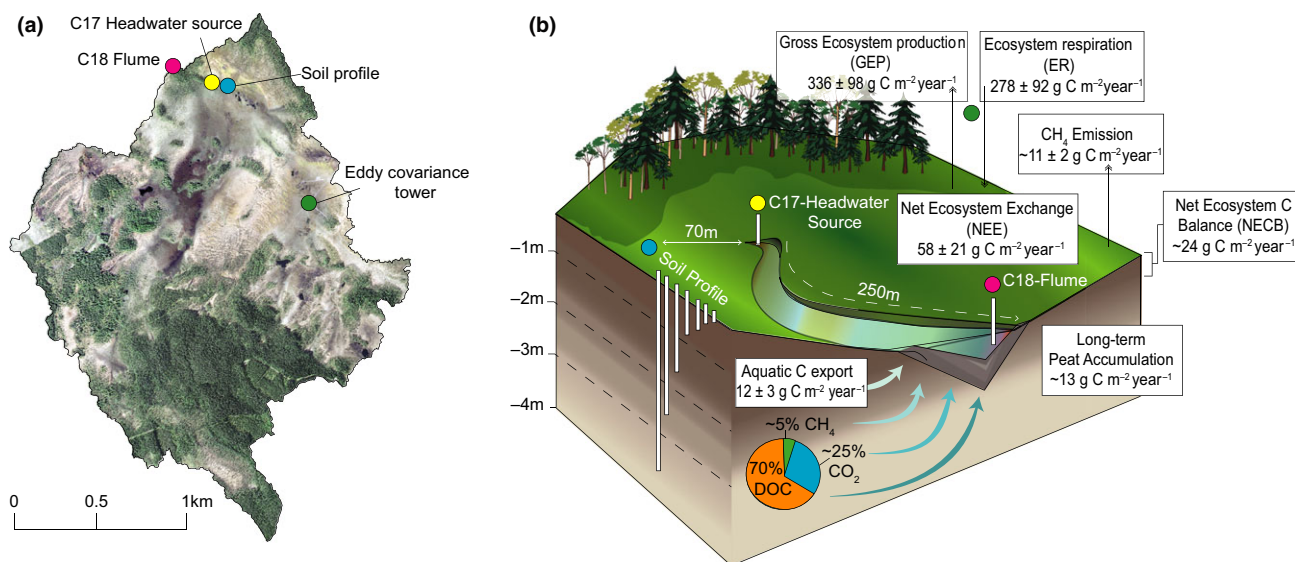


**FIGURE 1** (a) Map of Degerö Stormyr indicating the location of the two stream sampling stations C17 and C18, as well as the instrumented peat profile and the eddy-covariance tower (left). (b) Unscaled catchment scheme of the Net Ecosystem Carbon Budget (NECB) (Nilsson et al., 2008) representing the net ecosystem exchange (NEE), estimated based on a 12 year record of gross ecosystem production (GEP) and ecosystem respiration (ER) during 2001–2012 (Peichl et al., 2014). The aquatic C export was also estimated from a 12 year record of TOC, DIC, and CH<sub>4</sub> export from the stream at the C17-Headwater source and C18-Flume stations (2003–2014) (Leach et al., 2016). The long-term C accumulation was based on peat core dating from Larsson et al. (2016). The CH<sub>4</sub> emissions from the peat surface and contemporary peat accumulation were estimated based on a 2 year record presented in Nilsson et al. (2008) [Color figure can be viewed at [wileyonlinelibrary.com](http://wileyonlinelibrary.com)]

is 614 mm, of which 35% usually falls as snow, based on observations from the nearby (10 km) Svartberget climate station (Swedish University of Agricultural Sciences). The mean annual temperature is  $+1.8^{\circ}\text{C}$ , ranging from a maximum average of  $+14.7^{\circ}\text{C}$  in July and minimum average  $-9.5^{\circ}\text{C}$  in January (Laudon et al., 2013). Annual peak stream discharge at the mire outlet, as measured at the C-18 station, typically occurs during spring due to snow melt runoff. Large rain events during summer and autumn can also generate peak flows in some years. Winter is dominated by low flow conditions.

The contemporary net ecosystem carbon budget (NECB) at Degerö is estimated to be  $-24 \text{ g C m}^{-2} \text{ yr}^{-1}$  (Nilsson et al., 2008), while the estimated Holocene long-term average rate of peat C accumulation is  $13 \text{ g C m}^{-2} \text{ yr}^{-1}$ , pointing to a similar or higher NECB in current times compared with the Holocene average (Larsson et al., 2016; Figure 1b). The contemporary net ecosystem exchange (NEE, 2001–2012) is  $-58 (\pm 21) \text{ g C m}^{-2} \text{ yr}^{-1}$  (Peichl et al., 2014) and the combined C loss as CH<sub>4</sub> emission and total aquatic C export corresponds to about 50% of the NEE (Leach et al., 2016; Nilsson et al., 2008; Figure 1b). The vegetation covering the fen is dominated by lawns and carpet plant communities dominated by *Eriophorum vaginatum* L., *Trichophorum cespitosum* (L.) Hartm., *Vaccinium oxycoccos* L., *Andromeda polifolia* L., and *Rubus chamaemorus* L., with both *Carex limosa* L. and *Schezeria palustris* L. as well as sparse occurrence of *Carex rostrata*.

The studied stream is the outlet of a sub-catchment within the Degerö mire complex, draining a total area of  $2.7 \text{ km}^2$ , representing 40% of the total mire complex (Figure 1a). The fen covers 70% of the stream's catchment area, while the remaining 30% consists of

coniferous forest underlain by soils derived from glacial till, located in the periphery of the fen, as seen from LIDAR scan of the catchment, available in Leach et al. (2016). Water balance assessment indicates a low potential for hydrological sources coming from outside the delineated catchment area (Peichl et al., 2013). Runoff water generated within the nearest forested portion of the catchment must cross at least 950 m (horizontal distance) through the fen in order to reach the headwater source. During this transport, much of the original chemical character of this water from the podzolized mineral soils underlying the forest is likely lost, particularly its original C load, which is heavily supplemented by the fen. The two stream sampling stations (C17-Headwater Source and C18-Flume) are located 15 m and 250 m downstream from the stream initiation point, respectively (Figure 1). The stream initiation point is found in a zone of flow convergence where water under low hydraulic pressure is forced to the surface by the shallow depth (1 m) of the underlying mineral layer. The C18 station is equipped with a 10 m long trapezoidal flume inside a heated house where stage height measurements are made throughout the year (Figure 1). Stream discharge was determined by applying a stage height-discharge rating curve to hourly water level measurements. A theoretical rating curve for the flume was calibrated using manual discharge measurements made over a range of flow conditions.

To make continuous measurements of aquatic CO<sub>2</sub> concentrations, both stream stations were instrumented with Vaisala CARBOCAP GMP221 nondispersive infrared (NDIR) CO<sub>2</sub> sensors (range 0%–5%), which were enclosed with a water-tight, gas-permeable Teflon membrane (PTFE) and sealed with Plasti Dip (Plasti Dip international, Baine, MN, USA) to ensure that the sensor was protected

from water but remained permeable to gas (Johnson et al., 2010). Both stations were also instrumented with pressure transducers (MJK 1400, 0–1 m, MJK Automation AB) for water table height measurements and temperature sensors (TO3R, TOJO Skogsteknik) that recorded hourly. All continuously measured data were stored on external data loggers (CR1000, Campbell Sci.).

A set of seven groundwater wells was installed about 70 m from the stream initiation point in a zone of flow confluence where the total soil depth reaches 3–4 m (Figure 1b). The soil profile consists of accumulated peat in the top 3 m, which overlays a ca. 1 m thick layer of organic lake sediments (Larsson et al., 2016). Each groundwater well contained thin plastic tubing with taps allowing manual collection of peat pore water samples with syringes at specific depths across the peat profile. These wells were placed at different depths in the peat profile (0–0.25 m, 0.25–0.5 m, 0.5–1 m, 1–2 m, 2–3 m, 3–4 m) to sample potential hydrological flowpaths to the stream (Figure 1b).

## 2.2 | Stream and soil water chemistry analysis

Stream water samples were collected at both the C17 and C18 stream stations. Sampling was carried out on a monthly basis from November to April, two to three times a week during the freshet, and every second week between June and October, producing a total of 39 sampling occasions between May 2015 and June 2016. Peat pore water samples were collected monthly during the open water period (May–Oct 2015) on six separate occasions. The water samples were analyzed for gaseous components, including CO<sub>2</sub> and CH<sub>4</sub> concentration, as well as nongaseous components, DOC, DIC, and pH and stable isotope composition  $\delta^{13}\text{C}$ -DIC,  $\delta^{13}\text{C}$ -CH<sub>4</sub>, and  $\delta^{18}\text{O}$  (‰).

The CO<sub>2</sub> and CH<sub>4</sub> concentrations were measured from the same sample, using the acidified headspace method (Åberg & Wallin, 2014; Wallin, Buffam, Öquist, Laudon, & Bishop, 2010). The stream water DIC, CO<sub>2</sub>, and CH<sub>4</sub> concentrations were calculated from GC determined headspace  $p\text{CO}_2$  and  $p\text{CH}_4$  corrected for in situ stream pH and water temperature. The precision of sampling and analysis were estimated to an average of 10% (standard deviation (SD)), based on replicate sampling (Nilsson et al., 2008; Öquist, Wallin, Seibert, Bishop, & Laudon, 2009). The sensor-derived and manual spot measurements of stream water CO<sub>2</sub> concentration showed a close correspondence, with an average difference of –7% ( $t$ -test  $p = .61$ ). The detection limit for CH<sub>4</sub> concentration corresponded to 2.0  $\mu\text{g C L}^{-1}$  at a stream water temperature of 2°C and with the water-air volume ratio used (1 ppm CH<sub>4</sub> from the instrument). This limit was exceeded in all stream and soil water samples.

Samples for pH analysis were collected in 50 ml high-density polyethylene bottles, which were slowly filled and closed under water in order to avoid pockets of air in the bottle. The pH was measured in the laboratory using a Mettler Toledo MP 220 pH Meter with an accuracy of  $\pm 0.1$  units. The DOC concentration was analyzed from 10 ml of stream or peat pore water, filtered at 0.45  $\mu\text{m}$  in the field and stored in high-density polyethylene bottles. Previous analysis showed no statistically significant differences

between the filtered and unfiltered samples, indicating that DOC is a reasonable proxy for TOC (Laudon et al., 2011; Nilsson et al., 2008). Prior to analysis, samples were acidified and sparged to remove inorganic carbon. The samples were analyzed using a Shimadzu Total Organic Carbon Analyzer TOC-V<sub>CPH</sub>, following storage in 4°C refrigerators for 2–3 days periods (Leach et al., 2016).

Peat pore water samples and a subset of stream water samples were analyzed for  $\delta^{13}\text{C}$ -DIC and  $\delta^{13}\text{C}$ -CH<sub>4</sub>. Samples for  $\delta^{13}\text{C}$ -CH<sub>4</sub> analysis were collected in a 100 ml glass vial, filled completely with stream or peat pore water samples and closed airtight with a rubber septum. One ml of 50% w/v ZnCl<sub>2</sub> solution was injected in each glass vial directly after sample collection for preservation. Samples for the  $\delta^{13}\text{C}$ -DIC analysis were directly injected into 12 ml septum-sealed glass vials (Labco Limited) prefilled with N<sub>2</sub> gas, and preinjected with phosphoric acid in order to convert all DIC species to CO<sub>2</sub> (g). The samples for  $\delta^{13}\text{C}$  composition were analyzed using a Gasbench II and a Thermo Fisher Delta V mass spectrometer. The  $\delta^{13}\text{C}$  values are given in terms of deviation from the standard Vienna Pee-Dee Belemnite (VPDB). The repeated measurements of the standard indicated a standard deviation <0.2 ‰ on each sampling occasion. The water isotopes ( $\delta^{18}\text{O}$ ) were analyzed following the same procedure as Laudon, Sjöblom, Buffam, Seibert, and Morth (2007) and Peralta-Tapia, Sponseller, Tetzlaff, Soulsby, and Laudon (2015).

## 2.3 | Analysis and interpretation of <sup>14</sup>C-DOC, <sup>14</sup>C-CO<sub>2</sub>, and <sup>14</sup>C-CH<sub>4</sub>

During May 2015–June 2016, a total of 70 samples were collected and analyzed for <sup>14</sup>C content of DOC (<sup>14</sup>C-DOC), CO<sub>2</sub> (<sup>14</sup>C-CO<sub>2</sub>), and CH<sub>4</sub> (<sup>14</sup>C-CH<sub>4</sub>) in both stream and peat pore water. Sample collection for manual spot measurements of <sup>14</sup>C-DOC, <sup>14</sup>C-CO<sub>2</sub>, and <sup>14</sup>C-CH<sub>4</sub> were taken at the headwater source and at five different depths across the peat profile (0.25, 0.75, 1.5, 2.5, and 3.5 m below the surface of the mire) on three separate occasions, May (spring), August (summer), and October (autumn) 2015. The manual spot measurements of stream water <sup>14</sup>C-CO<sub>2</sub> were complemented with nine integrative measurements of <sup>14</sup>C-CO<sub>2</sub>, passively sampled using molecular sieve cartridge (MSC) traps located below the water surface, which slowly collect stream water CO<sub>2</sub> over extended time periods (Garnett, Hartley, Hopkins, Sommerkorn, & Wookey, 2009). These passive samplers were deployed for periods ranging from 4 to 8 weeks; collectively they cover more than a full year (May 2015–June 2016). The trapping capacity of the MSC was never exceeded (<100 ml CO<sub>2</sub>). Additional manual spot measurements of stream water <sup>14</sup>C-DOC were taken at each change of MSC, in order to characterize cumulative <sup>14</sup>C-DOC under a large range of hydrological conditions. The samples for analysis of stream water <sup>14</sup>C-CO<sub>2</sub> and <sup>14</sup>C-DOC were taken at the headwater source station (C17) during open water periods, but moved to the flume station (C18) during the ice-covered periods for accessibility. Simultaneous measurement of <sup>14</sup>C-CO<sub>2</sub> and <sup>14</sup>C-DOC at both stations in May 2015 showed close correspondence, with only a 0.2 and 0.5 %modern difference, respectively, within the range of measurements precision.

Manual spot measurements of  $^{14}\text{C}$ - $\text{CO}_2$  were carried out with the super headspace method whereby  $\text{CO}_2$  samples were collected onto MSCs [see Garnett, Billett, Gulliver, and Dean (2016) for further details]. The method for manual spot measurement of  $^{14}\text{C}$ - $\text{CH}_4$  followed a protocol similar to that for  $^{14}\text{C}$ - $\text{CO}_2$ , with the exception that the recovered gas volume was injected into 10 L foil bags (SKC Ltd, UK), rather than MSCs [see Garnett, Gulliver, and Billett (2016) for further details]. The  $^{14}\text{C}$ -DOC analysis was performed on 1 L soil and stream water samples collected in preacid-washed glass bottles. The samples were filtered in the laboratory through 0.7  $\mu\text{m}$  glass fiber filters. The time-integrated samples for determination of stream  $^{14}\text{C}$ - $\text{CO}_2$  and  $\delta^{13}\text{C}$ - $\text{CO}_2$  were achieved by deploying passive samplers [see Garnett et al. (2012) for further details]. The samplers were based on the MSCs described above, but attached with a gas-permeable hydrophobic filter [Accurel PP V8/2 HF tubing, Membrana GmbH, Germany (Gut et al., 1998)]. Radiocarbon results were expressed as %modern and conventional radiocarbon age (years before present (BP), where 0 BP = AD 1950), with  $\pm 1\sigma$  analytical precision. The atmospheric  $^{14}\text{C}$  concentration during the study period was assumed to be 102.5 %modern, in accordance with the empirical relationship from Levin, Hammer, Kromer, and Meinhardt (2008).

According to conventional  $^{14}\text{C}$  dating techniques, an average age can be assigned to each  $^{14}\text{C}$  value obtained from the previously described analysis. However, in  $^{14}\text{C}$  composite samples, for example gases or solutes, the  $^{14}\text{C}$  content potentially originates from multiple C source combinations with different  $^{14}\text{C}$ -ages. Thus, the average  $^{14}\text{C}$  age has no easily interpretable meaning. Here, we assumed that all samples with  $^{14}\text{C}$ -content >100 %modern contain a substantial component of postbomb C, fixed from the atmosphere post 1964. But it is worth noting that  $^{14}\text{C}$  contents <100 %modern do not preclude the presence of postbomb C. For example, a  $^{14}\text{C}$  content of 95 %modern is equivalent to a conventional  $^{14}\text{C}$  age of ~410 years BP. But, such  $^{14}\text{C}$  content can arise from an even mixture of two C pools at 120 %modern and 70 %modern. Alternatively, an even mixture now consisting of 93 %modern and 97 %modern, can result in the same total  $^{14}\text{C}$  content and age, yet incorporate no postbomb  $^{14}\text{C}$ . In light of these issues, we purposefully avoided reporting the measured  $^{14}\text{C}$  contents in terms of ages from conventional  $^{14}\text{C}$  dating. Instead, we focused our interpretation of  $^{14}\text{C}$  results using the relative differences in  $^{14}\text{C}$  contents between C forms or changes over time in order to draw conclusions on the sources and controls of dissolved C in stream and peat pore water.

The  $^{14}\text{C}$  content of the calibrated solid peat stratigraphy, obtained from Larsson et al. (2016), was also reported here for comparison with the  $^{14}\text{C}$ -content of the dissolved and gaseous C species. It is important to note that these  $^{14}\text{C}$ -contents were determined on plant fragments from mosses or aboveground vascular plant tissues to ensure a representative dating of the specific depth (Larsson et al., 2016; Nilsson et al., 2001; Figure 3a and Section S2). Both the hydrolyzable and fine fraction (<0.045 mm) of the peat core samples were removed from this  $^{14}\text{C}$  analysis. These fractions are known to be generally be more  $^{14}\text{C}$ -enriched than the age of

corresponding depth (Nilsson et al., 2001). For simplicity, we refer to these  $^{14}\text{C}$ -contents as the solid peat material.

## 2.4 | Stream $^{14}\text{C}$ export calculations and statistical analyses

Least-square regressions were performed to identify statistically significant relationships between different variables. These relationships were considered significant when  $p$ -values were <0.05. Mean values are presented in the text, along with standard deviations found within brackets. The best fit between antecedent discharge and  $^{14}\text{C}$ - $\text{CO}_2$  or  $^{14}\text{C}$ -DOC was determined by testing different time lags with 24 hr intervals up to a period of 2 weeks. The nonparametric Wilcoxon-test was used to determine statistical differences in water chemistry between the C17 and C18 stream stations. Analyses were performed using R Core Team (2013). R: A language and environment for statistical computing. R Foundation for Statistical Computing, Vienna, Austria. URL <http://www.R-project.org/>.

## 3 | RESULTS

### 3.1 | Stream C export and isotopic composition

The stream water DOC concentration at the headwater source, averaged 24.7 ( $\pm 4.6$ ) mg C L $^{-1}$  ( $n = 33$ ) during the 13 months' study period (May 2015–July 2016) and did not differ significantly from the downstream flume station ( $p = .68$ ), where the average concentration was 24.4 ( $\pm 5.1$ ) mg C L $^{-1}$  ( $n = 28$ ) (Figure 2a). The stream water  $\text{CO}_2$  concentration at the headwater source averaged 13.6 ( $\pm 5.7$ ) mg C L $^{-1}$  during the open water season (May–October,  $n = 4,583$  measured hourly), and was four times higher compared to the flume station ( $p < .0001$ ), where it averaged 6.2 ( $\pm 1.6$ ) mg C L $^{-1}$  ( $n = 9,703$ , measured hourly throughout the year; Figure 2a). The stream water  $\text{CH}_4$  concentration at the headwater source averaged 0.95 ( $\pm 1.2$ ) mg C L $^{-1}$   $n = 37$ ; these were also significantly higher than at the flume station, where the annual average concentration was 0.1 ( $\pm 0.1$ ) mg C L $^{-1}$   $n = 30$  (Figure 2a). The stream pH averages 4.5 ( $\pm 0.2$ )  $n = 10$  (Figure 5c).

The total aquatic C export at the headwater source station was estimated at 10.8 g C m $^{-2}$  yr $^{-1}$ , of which DOC export contributed 76% (8.2 g C m $^{-2}$  yr $^{-1}$ ), with  $\text{CO}_2$  and  $\text{CH}_4$  export representing 2.4 and 0.2 g C m $^{-2}$  yr $^{-1}$  (22% and 2%), respectively during the study year. The stream discharge ranged across nearly three orders of magnitude, from the lowest flow conditions at 0.5 L/s during the winter and summer, to peak flow conditions of 382 L/s during the spring freshet in April and May (Figure 2b). The average flow over the study period was 21.9 ( $\pm 40.1$ ) L/s. There was a significant negative relationship between the stream water concentration of all three C species and discharge over the studied period (Fig. S3). Spring freshet contributed 71% of the annual runoff, as well as 60% of the annual DOC export, 53% of the  $\text{CO}_2$  export, but only 26% of the annual  $\text{CH}_4$  export. Two major rain events occurred during the open water season, the first

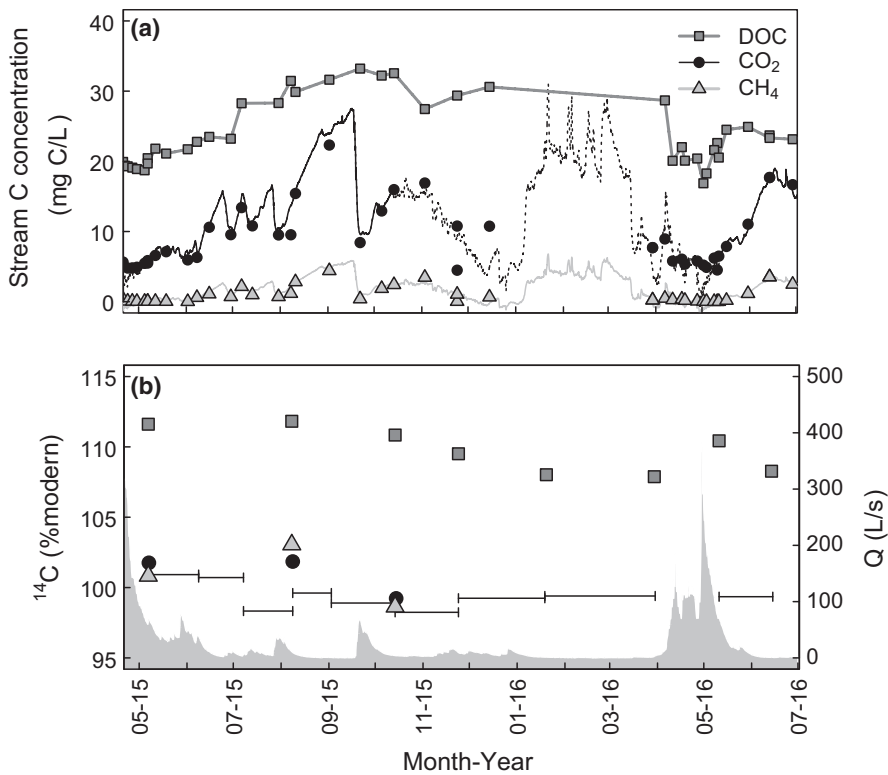


**FIGURE 2** (a) Time series of stream dissolved organic carbon (DOC) (gray squares),  $\text{CO}_2$  (black line and circles) and  $\text{CH}_4$  (light gray triangles) concentration at the headwater source location from May 2015 to July 2016, combining automated hourly and manual spot measurements. The full black line represents the hourly measured  $\text{CO}_2$  concentrations, while the dotted black line represents the estimated hourly  $\text{CO}_2$  concentrations during winter (Equation S1). The gray line represents the estimated hourly  $\text{CH}_4$  concentrations (Equation S2). (b) Time series of stream discharge (gray area) expressed in L/s, and the stream water  $^{14}\text{C}$ -DOC (gray squares),  $^{14}\text{C}$ - $\text{CO}_2$  (black circles (manual spot measurement) and horizontal bars (time-integrated measurements)) and  $^{14}\text{C}$ - $\text{CH}_4$  (light gray triangles) expressed in %modern between May 2015 and June 2016

in late July (peak flow = 40.8 L/s) and the second in late September (peak flow = 70.9 L/s). Together, they contributed ca 10% of the annual runoff as well as 13%, 16%, and 23% of DOC,  $\text{CO}_2$ , and  $\text{CH}_4$  annual export, respectively.

The stream water  $^{14}\text{C}$ - $\text{CO}_2$ , derived from time-integrated samples, varied from 100.9% to 98.2 %modern over the complete annual cycle ( $n = 7$ ) (Figure 2b, Table S1). The stream water  $^{14}\text{C}$ - $\text{CO}_2$ , derived from manual spot measurements, was within the same range of values, with 101.8–99.2 %modern ( $n = 3$ ) (Figure 2b, Table S2). The stream water  $^{14}\text{C}$ - $\text{CH}_4$ , derived from manual spot measurements ( $n = 3$ ), varied from 103.1 to 98.6 %modern (Figure 2b, Table S2).

The stream water  $^{14}\text{C}$ -DOC was consistently enriched with post-bomb C throughout the hydrological year, ranging from 111.8 %modern to 107.9 %modern ( $n = 8$ ) (Figure 2b, Table S2). There was a persistent gap of ca 10 %modern between the stream water  $^{14}\text{C}$ - $\text{CO}_2$  and  $^{14}\text{C}$ -DOC across the whole year, with DOC being consistently more enriched with postbomb C compared to  $\text{CO}_2$  (Figure 2b).

The stream water  $\delta^{13}\text{C}$ -DIC values averaged  $-11.5\text{‰}$  ( $\pm 4.6$ )  $n = 6$ , while the  $\delta^{13}\text{C}$ - $\text{CH}_4$  values averaged  $-71.9\text{‰}$  ( $\pm 14.1$ )  $n = 6$ . The apparent isotopic fractionation factor between  $\text{CO}_2$  and  $\text{CH}_4$  ( $\alpha_{\text{CO}_2\text{-CH}_4}$ ) in the stream averaged 1.065, but varied across a large range, from  $\alpha = 1.035$ – $1.083$  (Figure 3c). The seasonal variability in stream  $\delta^{13}\text{C}$ -DOC was low, with an average of  $-28.4\text{‰}$  ( $\pm 0.60$ ) ( $n = 7$ ) (Table S2).

### 3.2 | Peat profile characteristics, C concentration, and isotopic composition

The water table position averaged  $-0.3$  cm below the surface at the location of the soil depth profile during the studied period. The water

table position reached a minimum of  $-12$  cm during the driest period of the summer and a maximum of  $+22$  cm during the snow melt. The dry bulk density of the soil profile averaged  $0.06$  ( $\pm 0.1$ )  $\text{g}/\text{cm}^3$  with the lowest bulk density of  $0.001$   $\text{g}/\text{cm}^3$  at  $-2.5$  m depth and the highest density point at  $0.73$   $\text{g}/\text{cm}^3$  just above bedrock, at a depth of  $-4$  m in the organic lake sediments layers (Fig. S4). The pH across the depth profile averages  $4.3$  ( $\pm 0.3$ )  $n = 38$  (Figure 5). The concentration of all three C species (DOC,  $\text{CO}_2$ , and  $\text{CH}_4$ ) followed a convex distribution along the peat profile, with the lowest concentrations observed at both the top and bottom of the profile ( $0$ – $0.5$  m;  $-2$  to  $4$  m), while the highest concentrations were found in the middle section of the peat profile ( $-1.5$  m) (Figure 3a). Peat pore water DOC concentrations across the full depth peat profile averaged  $40.8$  ( $\pm 12.0$ )  $\text{mg C L}^{-1}$  ( $n = 38$ , 6 depths, 6 occasions; Figure 3b). The  $\text{CO}_2$  concentrations across the full depth peat profile were comparable to the DOC concentrations, averaging  $36.5$  ( $\pm 21.8$ )  $\text{mg C L}^{-1}$  ( $n = 38$ , 6 depths, 6 occasions; Figure 3b). The similarity of DOC and  $\text{CO}_2$  concentrations was particularly strong in the top 2 m of the peat profile (Figure 3b). The  $\text{CH}_4$  concentrations averaged  $5.3$  ( $\pm 2.6$ )  $\text{mg C L}^{-1}$  across the full depth peat profile ( $n = 34$ , 6 depths, 6 occasions). The  $\text{CO}_2$ : $\text{CH}_4$  ratio was near 8:1 in the upper 2 m of the peat profile, but decreased to 4:1 in the lower 2 m (Figure 3b).

Peat pore water  $^{14}\text{C}$ - $\text{CO}_2$  and  $^{14}\text{C}$ - $\text{CH}_4$  followed a progressive decline with depth across the peat profile (Figure 3a). The highest  $^{14}\text{C}$ - $\text{CO}_2$  and  $^{14}\text{C}$ - $\text{CH}_4$  values were found within the top 0.5 m of the peat profile, with an average of 107.1 and 108.8 %modern, respectively (Figure 3a). The lowest  $^{14}\text{C}$ - $\text{CO}_2$  and  $^{14}\text{C}$ - $\text{CH}_4$  values were found in the bottom 2–4 m of the peat profile, averaging 96.9 and 98.9 %modern, respectively (Figure 3). The  $^{14}\text{C}$ - $\text{CO}_2$  and

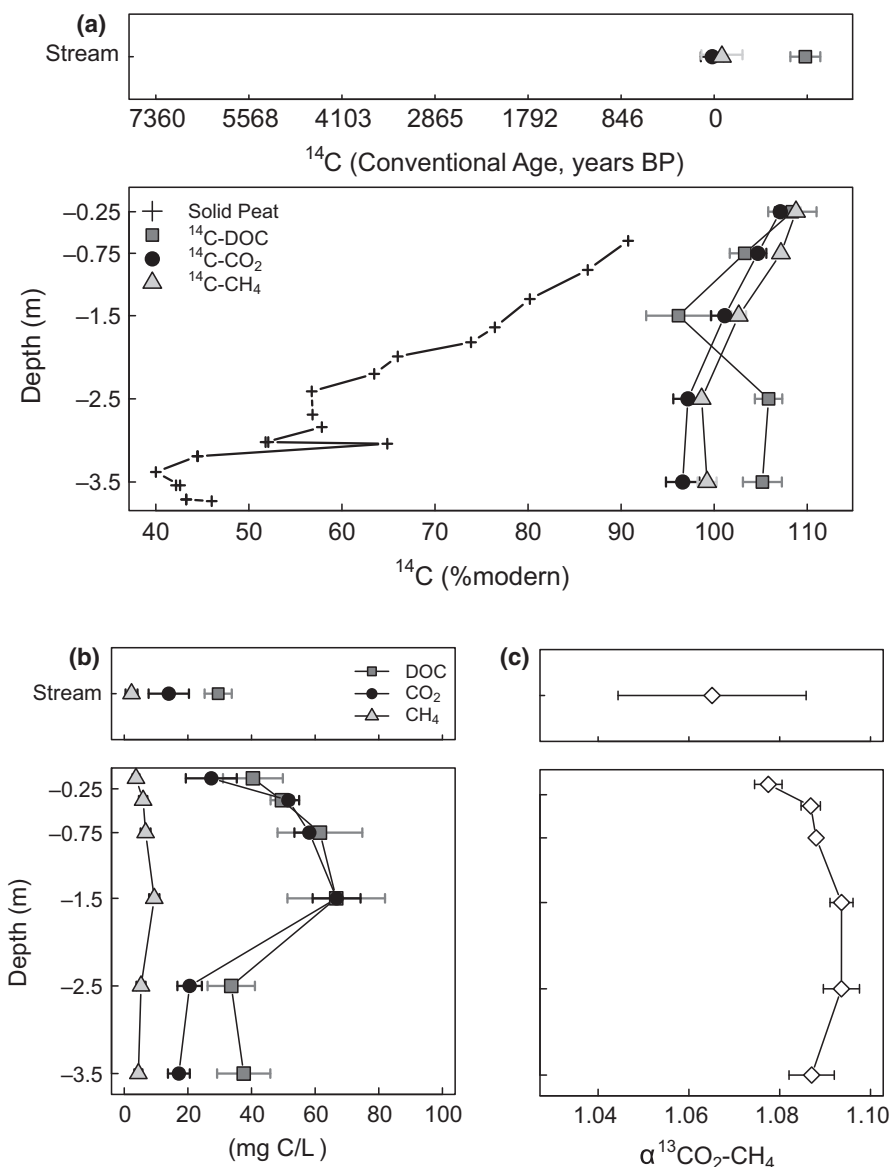


**FIGURE 3** Stream and peat depth profile of (a) the average  $^{14}\text{C}$ -content of different C fractions, expressed in % modern and conventional  $^{14}\text{C}$  ages (top panel), (b) C concentration (bottom left panel) and (c)  $\alpha_{\text{CO}_2\text{-CH}_4}$  (bottom right panel). The top boxes on each panel represent the stream, while the main boxes represent the peat depth profile. Each point represents average values, with gray squares representing dissolved organic carbon (DOC), black circles CO<sub>2</sub> and light gray triangles CH<sub>4</sub>, and bars representing the standard deviation. Black crosses in the top panel represent the  $^{14}\text{C}$  content of the solid peat material taken from Larsson et al. (2016)

$^{14}\text{C}$ -CH<sub>4</sub> were very similar across all sampling locations and periods, with an average difference of only  $\pm 1.9$  %modern, with CH<sub>4</sub> being consistently more enriched in  $^{14}\text{C}$  than CO<sub>2</sub> (Figures 3a and 4a). As a result, there was a highly significant positive relationship between  $^{14}\text{C}$ -CO<sub>2</sub> and  $^{14}\text{C}$ -CH<sub>4</sub>, including all simultaneous  $^{14}\text{C}$  measurements in stream and peat pore water (Figure 4a).

$$^{14}\text{C-CH}_4 = 6.3 + ^{14}\text{C-CO}_2 \times 0.9 \quad R^2 = 0.89, n = 18, p < 0.0001 \quad (1)$$

Both the  $\delta^{13}\text{C}$ -DIC and  $\delta^{13}\text{C}$ -CH<sub>4</sub> values were highly variable across the peat profile, with an average of  $-4.1$  ‰ ( $\pm 4.8$ )  $n = 37$  and  $-83.2$  ‰ ( $\pm 5.7$ ) (SD)  $n = 38$ , respectively. The  $\alpha_{\text{CO}_2\text{-CH}_4}$  across the peat profile averaged  $\alpha = 1.086$  ( $\pm 0.009$ )  $n = 38$ , with the lowest average ratio near the surface ( $\alpha = 1.078$ ) and the highest average ratio at  $-2.5$  m ( $\alpha = 1.093$ ; Figure 3c).

The  $^{14}\text{C}$ -DOC across the peat profile differed markedly from the  $^{14}\text{C}$ -CO<sub>2</sub> and  $^{14}\text{C}$ -CH<sub>4</sub>, both in terms of overall  $^{14}\text{C}$  content and vertical enrichment within the peat profile (Figure 3a). The  $^{14}\text{C}$ -DOC

had a substantial proportion of postbomb C, with most enriched  $^{14}\text{C}$ -DOC found in the top and bottom of the peat profile (0–0.5 m and 2–4 m), where the  $^{14}\text{C}$ -DOC averaged 108.4 and 105.5 %modern, respectively (Figure 3a). The least enriched  $^{14}\text{C}$ -DOC was found in the middle section of the peat ( $-1.5$  m), where the  $^{14}\text{C}$ -DOC averaged 96.2 %modern (Figure 3a). There was a significant negative relationship between the soil and stream water  $^{14}\text{C}$ -DOC (%modern) and the DOC concentration (mg C L<sup>-1</sup>) (Figure 4b).

$$^{14}\text{C-DOC} = 117.5 + \text{DOC} \times -0.3 \quad R^2 = 0.69, n = 20, p < 0.0001 \quad (2)$$

The  $\delta^{13}\text{C}$ -DOC values in the peat pore water averaged  $-27.9$  ‰ ( $\pm 0.7$ ) across the full depth peat profile ( $n = 16$ ), with slightly more positive values between 0.5 and 1 m, but more negative values near the surface (0.25 m) and the bottom of the peat profile (2–4 m). There was an overall significant negative relationship between soil and stream water  $^{14}\text{C}$ -DOC (%modern) and  $\delta^{13}\text{C}$ -DOC (‰):

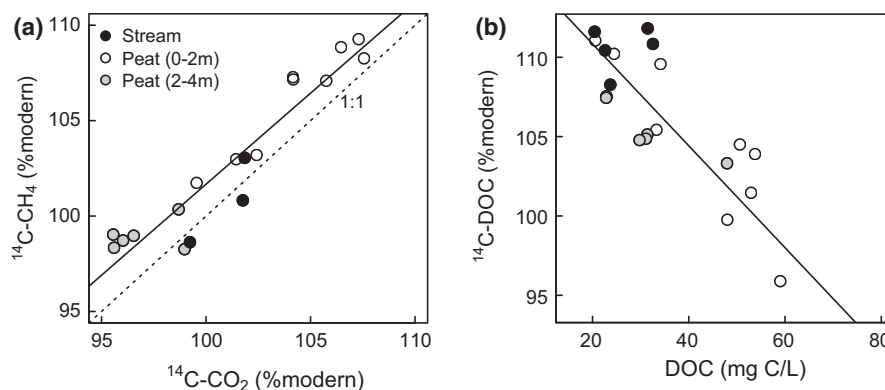


**FIGURE 4** Scatterplot showing the least-square regression model (full line) between (a)  $^{14}\text{C-CO}_2$  and  $^{14}\text{C-CH}_4$  (Equation 1) with dotted line representing the 1:1 ratio, and (b)  $^{14}\text{C-DOC}$  and DOC concentration (Equation 2), including both peat pore water and stream water. Peat pore water samples are separated into two groups, samples from 0 to 2 m (white circles), and from 2 to 4 m (gray circles), while stream water samples are represented by black circles

$$^{14}\text{C-DOC} = -28.2 + \delta^{13}\text{C-DOC} \times -4.8 \quad R^2 = 0.40, n = 24, p = 0.0006 \quad (3)$$

The  $^{14}\text{C}$  content of the different C species observed in the stream matched most closely that of the bottom two meters of the peat profile. A similar agreement between the chemical characteristics of the stream water and that of the bottom 2–4 m of the peat profile was observed in the patterns of  $\delta^{18}\text{O}$  values, pH, and water temperature (Figures 5, S5 and S6). Through these different inferences, we determined that the deep peat horizon (2–4 m) may contribute on average to 70% of the stream flow generation (Fig. S7).

### 3.3 | Controls on stream intra-annual variability in $^{14}\text{C}$ -content

There were significant relationships between stream discharge (L/s) and  $^{14}\text{C-CO}_2$  as well as  $^{14}\text{C-DOC}$  (%modern) across the entire study year, albeit with a –9 days' time lag ( $\log(Q_{-9d})$ ; Figure 6):

$$^{14}\text{C-CO}_2 = 96.7(SE \pm 0.8) + \log(Q_{-9d}) \times 1.0(SE \pm 0.3) \\ R^2 = 0.60, n = 11, p = 0.003 \quad (4)$$

$$^{14}\text{C-DOC} = 107.9(SE \pm 0.6) + \log(Q_{-9d}) \times 0.7(SE \pm 0.2) \\ R^2 = 0.61, n = 8, p = 0.01 \quad (5)$$

The predictability of  $^{14}\text{C-CO}_2$  values and  $^{14}\text{C-DOC}$  values was considerably improved by adding a time lag (Figure 6c). The  $R^2$  was 0.12 and 0.46 respectively for synchronic discharge ( $t = 0$ ), and increased to 0.60 when the 9 days' antecedent discharge ( $t = -216$  hr) was used (Figure 6c).

## 4 | DISCUSSION

### 4.1 | Intra-annual variability in $^{14}\text{C}$ content of aquatic C export

Contrary to our original hypothesis, the stream water  $^{14}\text{C-DOC}$ ,  $^{14}\text{C-CO}_2$ , and  $^{14}\text{C-CH}_4$  was highly influenced by postbomb C, with

relatively stable  $^{14}\text{C}$  content in both stream and soil waters over the study year (Figures 2b and 3a). Other studies reported similar total  $^{14}\text{C-DOC}$  content and intra-annual variability in streams from peat-dominated catchments, indicating a regular occurrence of young material in aquatic DOC export (Palmer, Hope, Billett, Dawson, & Bryant, 2001; Schiff et al., 1997; Tipping et al., 2010). Few studies have repeatedly characterized  $^{14}\text{C-CO}_2$  in stream water over time, but a study from a Scottish peatland reported a similar intra-annual variability in the  $^{14}\text{C}$  content, but with a much lower  $^{14}\text{C}$  content, resulting in both older and wider span in  $^{14}\text{C}$  content (from 91.6 to 86.0 %modern; Garnett et al., 2012). Together, our results indicate that the sources of the different C species sustaining aquatic C export are relatively similar throughout the year and largely contain recently fixed C from the atmosphere (postbomb, i.e. 1964). This apparently constant  $^{14}\text{C}$  source occurs despite considerable fluctuations in hydroclimatic conditions and C concentration in the stream (Figure 2a,b), which are known to affect both metabolic pathways and hydrological flowpaths delivering C to streams, both at this (Leach et al., 2016) and other mire sites (Dinsmore, Billett, & Dyson, 2013; Wilson et al., 2016; Winterdahl, Laudon, Lyon, Pers, & Bishop, 2016).

While the stream water  $^{14}\text{C-CO}_2$  and  $^{14}\text{C-CH}_4$  were similar across measurements, there was a persistent gap of ~10 %modern between the  $^{14}\text{C-DOC}$  and that of the gaseous C forms (Figure 2b). Such disparity in  $^{14}\text{C}$  content clearly indicates major differences in source material and formation processes, and/or transport mechanisms delivering the different C forms to the stream. Other studies have reported a higher content of postbomb C in stream DOC relative to aquatic  $\text{CO}_2$ , which could be explained by the influence of carbonate minerals dissolution generating DIC (Billett et al., 2007; Leith et al., 2014; Tipping et al., 2010). To our knowledge, such DIC sources are absent in the Degerö Stormyr catchment, according to the bedrock composition and the molar Ca:Na in streams in the area (averaging  $0.58 \pm 0.12$ ; Laudon et al., 2013). Therefore, our results indicate that large differences in  $^{14}\text{C}$  content between DOC and gaseous C forms in streams can persist even in catchments with strict biogenic C sources.



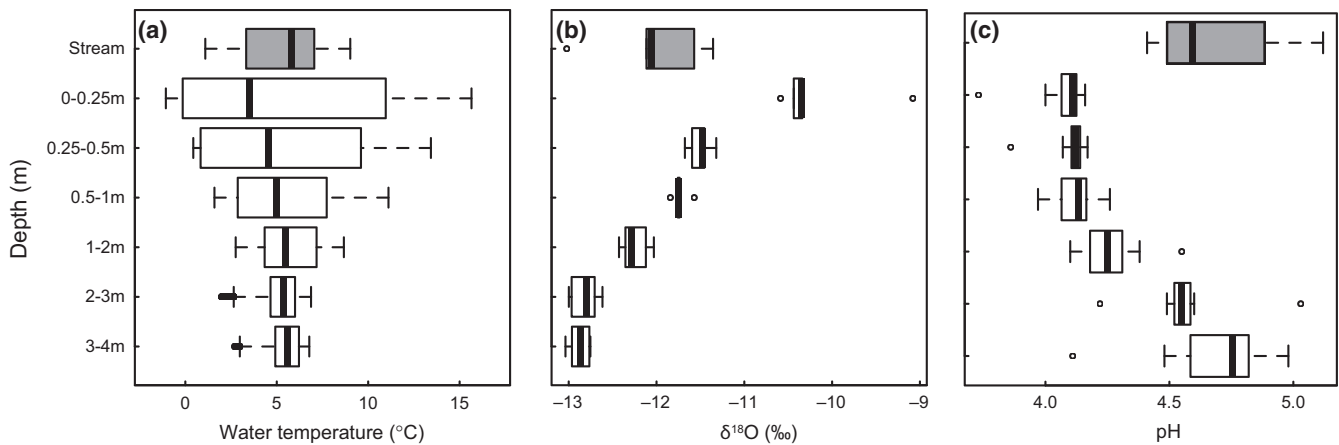


**FIGURE 5** Boxplots summarizing the (a) water temperature (°C) (b)  $\delta^{18}\text{O}$  values (‰) and (c) pH at different sampling locations starting from the top with the stream and followed by the peat depth profile. Boxes represent the median, and lower and upper quartiles (25% and 75%), while the whiskers show the 95% percentiles with minimum and maximum values shown as circles

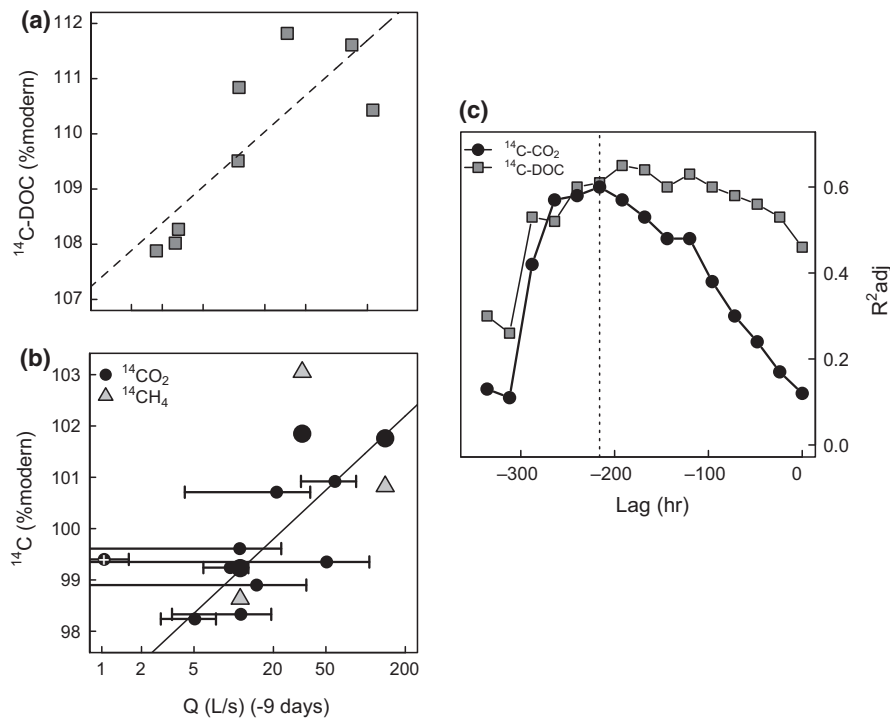


**FIGURE 6** Scatterplots showing the relationship between the antecedent stream discharge (9 days earlier), expressed in L/s and using a logarithmic scale and (a) the stream water  $^{14}\text{C-DOC}$  (gray squares), and (b) the  $^{14}\text{C-CO}_2$  (black circles), expressed in %modern, with the full lines representing the least-square linear regression model (Equations 4 and 5). In panel (b), the light gray triangles represent the  $^{14}\text{C-CH}_4$ , the large black circles represent manual spot measurements of  $^{14}\text{C-CO}_2$ , and the small black circles represent the time-integrated measurements of  $^{14}\text{C-CO}_2$ , with bars representing the standard deviation of the discharge over the measurement period. The black dot with a white cross represents the time-integrated  $^{14}\text{C-CO}_2$  measurement taken from January to March, which was considered an outlier. (c) scatterplot showing the  $R^2$  of individual least-square linear regression models between  $^{14}\text{C-DOC}$  (gray squares) or  $^{14}\text{C-CO}_2$  (black circles) and stream discharge under different lag periods starting from  $t = 0$ , up to 2 weeks earlier, with the dotted line highlighting the best fit, found at  $-9$  days' lag period

The  $^{14}\text{C}$  characterization of DOC,  $\text{CO}_2$ , and  $\text{CH}_4$  down the peat profile also allowed to determine that a major flowpath for the aquatic C export occurs through the bottom 2–4 meters of the peat profile, where the  $^{14}\text{C}$  content of the three different C forms matches most closely that of the same C species in the stream (Figure 3a).

The intra-annual variability in stream water  $^{14}\text{C-CO}_2$  is best explained by a constant supply of C from the deep peat layers (2–4 m; averaging 70% of the annual export), supplemented with superficial flowpaths during high-flow events (0–25 cm; Fig. S7). The peat bulk density profile also demonstrates a clear decrease in peat

density at 2 m depth (Fig. S4), suggesting the presence of macropores or preferential flowpaths with increased hydrological conductivity at this specific depth. In addition, the relationship between stream discharge and DOC, CO<sub>2</sub> and CH<sub>4</sub> concentrations demonstrated that stream C concentrations agree best with the bottom 2–4 m of the peat profile during base flow conditions (Fig. S3). All of these inferences were further supported by the patterns in water stable isotopes ( $\delta^{18}\text{O}$ ), pH, and water temperatures (Figures 5, S5 and S6). This interpretation of the sources of aquatic C export agrees well with the proposed hydrological model for the same catchment from Leach et al. (2016). Several studies have suggested that superficial flowpaths dominate the runoff generation in peatlands, with deep soil horizons often mostly hydrologically inactive (Ingram, 1982; Ronkanen & Kløve, 2007; Tipping et al., 2010), a conception that is clearly challenged by our results and those of others (Glaser et al., 2016; Holden & Burt, 2003) including a nearby peatland catchment (Laudon et al., 2007; Peralta-Tapia et al., 2015).

## 4.2 | Sources of DOC, CO<sub>2</sub>, and CH<sub>4</sub> across the peat profile

The <sup>14</sup>C-DOC, <sup>14</sup>C-CO<sub>2</sub>, and <sup>14</sup>C-CH<sub>4</sub> across the peat profile deviated considerably from the <sup>14</sup>C content of the solid peat material (Figure 3a). Both the <sup>14</sup>C-CO<sub>2</sub> and <sup>14</sup>C-CH<sub>4</sub> decreased with depth, by ca. –3 %modern per meter, which is much lower than the drop in <sup>14</sup>C content observed in the bulk solid peat (~20 %modern per meter; Figure 3a). The <sup>14</sup>C-CO<sub>2</sub> and <sup>14</sup>C-CH<sub>4</sub> near the surface of the peat profile (–25 cm; averaging 107.1 and 108.8 %modern, respectively), also deviated significantly from the atmospheric <sup>14</sup>C content during the studied period (102.5 %modern; Figure 3a). This suggests that direct root respiration is unlikely to be the sole source sustaining gaseous C concentrations near the peat surface. Instead, the <sup>14</sup>C content of CO<sub>2</sub>, CH<sub>4</sub> was most similar to the <sup>14</sup>C-DOC at that depth (Figure 3a), suggesting that a substantial fraction of the near surface gases is derived from DOC mineralization.

The close similarity in <sup>14</sup>C content between CO<sub>2</sub> and CH<sub>4</sub> in both peat pore water and stream water is a clear indication of the shared sources and transport processes controlling both gases (Figure 4a, Equation 1; Chanton et al., 2008; Clymo & Bryant, 2008; Garnett, Hardie, & Murray, 2011). Other studies have reported considerably larger differences in <sup>14</sup>C content between CO<sub>2</sub> and CH<sub>4</sub> in peat pore water or associated streams, which has been linked to disparity in sources or geological influences on either CO<sub>2</sub> or CH<sub>4</sub> (Chasar, Chanton, Glaser, Siegel, & Rivers, 2000; Garnett et al., 2013; Leith et al., 2014). The  $\alpha_{\text{CO}_2\text{-CH}_4}$  value in all peat pore waters (ranging from 1.047 to 1.10), suggested a persistent dominance of hydrogenotrophic methanogenesis, in contrast to acetoclastic methanogenesis, as the main metabolic pathway within the entire peat profile (Whiticar, Faber, & Schoell, 1986; Figure 3c). The dominance of hydrogenotrophic methanogenesis may explain the significant positive relationship between the <sup>14</sup>C content of both gases (Figure 4a, Equation 1).

The slope of this relationship (0.9) is similar to that reported from other peatlands (Chanton et al., 2008). Both methanogenic pathways are known to occur in peatlands, sometimes co-existing and shifting with seasons (Hornibrook, Longstaffe, & Fyfe, 2000; Throckmorton et al., 2015). However, hydrogenic methanogenesis seems to be the dominant pathway in acidic and nutrient-poor ecosystems, which characterizes well this poor fen (Bellisario et al., 1999; Holmes, Chanton, Tfaily, & Ogram, 2015; Kotsyurbenko et al., 2004). Despite the similarities between the <sup>14</sup>C-CO<sub>2</sub> and <sup>14</sup>C-CH<sub>4</sub> content, there was also a small but persistent gap in <sup>14</sup>C content of the two gases, with CH<sub>4</sub> being slightly <sup>14</sup>C-enriched (ca. 2 %modern) relative to CO<sub>2</sub>, yielding an intercept of +6 for this relationship. This intercept is noticeably more positive than reported from other peatlands (from –9 to –23) (Chanton et al., 2008; Figure 4a), which likely reveal differences in the source material contributing to the both C gases across catchments. In our case, this systematic gap in <sup>14</sup>C content between CO<sub>2</sub> and CH<sub>4</sub> could be explained by a comparatively larger input of atmospheric CO<sub>2</sub> through direct root respiration or by degradation of root exudates in the CO<sub>2</sub> pool.

The <sup>14</sup>C-DOC profile followed a very different pattern with depth compared to both CO<sub>2</sub> and CH<sub>4</sub> and the <sup>14</sup>C-content of the solid peat (Figure 3a). The DOC was most <sup>14</sup>C-enriched, with clear evidence of a postbomb C (>100 %modern) contribution both near the surface and at the bottom of the peat profile. At the middle of the profile (1.5 m below surface), the DOC was consistently <sup>14</sup>C-depleted during each of the three sampling occasions (Figure 3a). To our knowledge, such a convex distribution of <sup>14</sup>C-DOC across the peat profile has not been documented in other studies. Instead, most studies report progressive decreases in <sup>14</sup>C content of the DOC with peat depth (Chasar et al., 2000; Clymo & Bryant, 2008; Schiff et al., 1997). The convex <sup>14</sup>C-DOC distribution with depth persisted over all three sampling occasions, suggesting regular transport of postbomb DOC near the surface and bottom of the peat profile. The relationship between <sup>14</sup>C-DOC and DOC concentrations or  $\delta^{13}\text{C}$ -DOC was yet another indication of the importance of mass flow of DOC within the peat profile (Figure 4b, Equations 2 and 3). To our knowledge, similar relationships have not been explicitly reported in the current literature. Mixing of two major DOC pools could explain these relationships, where DOC accumulates in horizons where mass flow is low and incorporates some of the <sup>14</sup>C and  $\delta^{13}\text{C}$  of the surrounding solid peat. In comparison, <sup>14</sup>C-CO<sub>2</sub> and <sup>14</sup>C-CH<sub>4</sub> were unrelated to the total concentrations of CO<sub>2</sub> and CH<sub>4</sub> respectively, and varied across a slightly narrower range of <sup>14</sup>C content than <sup>14</sup>C-DOC, indicating a more constant supply from a dominant source.

While it is known that dissolved and gaseous C forms can be subject to different transport processes across the peat profile (e.g. mass flow, advection, and diffusion) (Chanton et al., 2008; Clymo & Bryant, 2008; Flury, Glud, Premke, & Mcginnis, 2015), the exact processes leading to the reported <sup>14</sup>C patterns across peat depths remain to be fully resolved. More in depth hydrological studies are needed to determine more clearly the origin of the C found across

this peat depth profile. The peat profile characterized here is found at a hydrological confluence of multiple flowpaths. The large C concentrations and noticeable influence of hydrogenotrophic methanogenesis are strong indications that the C traveling through the peat, as well as exported to the stream, originates from the fen itself, and not the forested sections on the periphery of the catchment. The  $\delta^{18}\text{O}$  water isotopes and temperature also demonstrated that the water circulating through the deeper peat layers is well mixed, suggesting an amalgamation of different C source areas within the fen (Figs. S5 and S6).

Overall, the mineralization of solid peat material from deep horizons appears to play a minor role in the production of dissolved C in the peat, particularly near the surface and bottom of the peat profile (Figure 3a, Section S2). Our results clearly suggest that organic substrates, derived from recently fixed C from the atmosphere (<60 years), contribute significantly to sustaining DOC,  $\text{CO}_2$ , and  $\text{CH}_4$  concentrations across the peat profile and in the stream (Figures 2b and 3a). Other studies have also reported large isotopic disconnects between the dissolved C species and the surrounding solid peat (Aravena et al., 1993; Chanton et al., 1995, 2008; Charman, Aravena, Bryant, & Harkness, 1999; Chasar et al., 2000; Clymo & Bryant, 2008; Corbett et al., 2013; Glaser et al., 2016; Schiff et al., 1998), but those differences are typically smaller than the ones reported in this study. Several of these studies have compared results from bogs and fens, leaving some indications that fens could contain comparatively younger dissolved C likely reflecting their differences in hydrological controls (Bellisario et al., 1999; Chanton et al., 1995, 2008; Corbett et al., 2013; Glaser et al., 2016). The underlying causes of these contrasting patterns in dissolved  $^{14}\text{C}$  content across peatlands have yet to be explained, but the degree of anthropogenic pressure is likely a key factor controlling the mobilization of ancient C stocks (Butman et al., 2014; Evans et al., 2014; Moore et al., 2013). Peatland systems are also well recognized for their diversity in terms of genesis and biogeochemistry, so further studies at other poor fens may reveal similar patterns to the ones reported here.

### 4.3 | Controls on aquatic $^{14}\text{C}$ export and implications for peat C stock stability

The intra-annual variability in stream water  $^{14}\text{C}$ -DOC and  $^{14}\text{C}$ - $\text{CO}_2$  was best explained by stream discharge, albeit with a significant time delay (Figure 6, Equations 4 and 5). This relationship likely reflected shifts in contributing flowpaths, delivering C to the stream with a higher modern fraction during high-flow periods associated with superficial flowpaths (0–25 cm) and with more  $^{14}\text{C}$ -depleted C exported during base flow conditions where contributions from deeper flowpaths dominate (2–4 m) (Fig. S7). The clear improvement of the explanatory power of discharge on  $^{14}\text{C}$ - $\text{CO}_2$  and  $^{14}\text{C}$ -DOC with a lag time of up to 9 days possibly suggests differences in hydrological conductivity between the source areas feeding aquatic C export (Figure 6c). These differences may cause the increase in stream discharge to occur before the resulting increase in  $^{14}\text{C}$  content, suggesting that the deeper and more  $^{14}\text{C}$ -depleted source area (2–4 m) responds faster to increasing runoff than the surficial and more  $^{14}\text{C}$ -enriched source area. A similar discharge-dependent relationship was also observed for a Scottish peatland stream, where the modern fraction of C export also increased during high-flow events, but without a noticeable time delay (Garnett et al., 2012). Our characterization of stream  $^{14}\text{C}$ - $\text{CO}_2$  and  $^{14}\text{C}$ -DOC also extended over the ice-covered season, a period of the year so far uncharacterized in northern peatlands. One stream water  $^{14}\text{C}$ - $\text{CO}_2$  sample, collected during the lowest winter flow conditions (Jan–March), was identified as an outlier in the relationship with discharge, since it had a higher post-bomb C content than predicted (Figure 6b). It is likely that the sources of  $\text{CO}_2$  within the peat profile and hydrological flowpaths delivering C to the stream during winter conditions differ compared with other seasons, but the exact processes leading to such shifts remain to be determined. Nonetheless, our results suggested no major changes in the source of aquatic C export between the ice-free and ice-covered season.

The flow conditions that occurred during our study captured 99.5% of the long-term flow variability observed at Degerö Stormyr

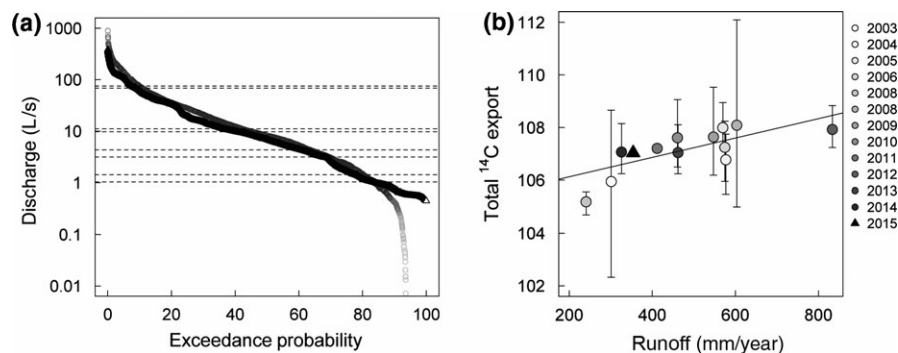


**FIGURE 7** (a) Flow duration curve of the stream for each year between 2003 and 2014 (circles in gray scales) and during the study year (black triangle; 2015), with flow conditions at the time of stream water  $^{14}\text{C}$ -DOC sample collection identified as dotted lines. (b) the estimated annual weighted average  $^{14}\text{C}$  content of total C export (Total  $^{14}\text{C}$  exp) for each year between 2003 and 2016, in relation to the annual runoff expressed in mm, with the bars representing the uncertainty of each prediction, and the solid line representing the least-square linear regression model (Total  $^{14}\text{C}$  exp =  $105.2 + \text{Runoff} \times 0.004$ ,  $R^2 = 0.53$ ,  $n = 12$ ,  $p = .004$ )

(0–901 L/s) (2003–2016) (Figure 7a; Leach et al., 2016). However, the most extreme flow conditions were not characterized in our stream  $^{14}\text{C}$  sampling (>75 L/s, 90% exceedance), thus representing a source of uncertainty (Figure 7a). Nonetheless, the observed relationship between the stream  $^{14}\text{C}$ -DOC and  $^{14}\text{C}$ - $\text{CO}_2$  and discharge spanned nearly the full range of  $^{14}\text{C}$  content characterized across the peat profile, indicating low potential for alternative C sources contributing to the C export under more extreme flow conditions (Figures 2b, 3a, and 6). We estimated the possible inter-annual variability in the  $^{14}\text{C}$  export (see details in Section S1), based on the two empirical relationships (Equations 4 and 5) and the long-term (2003–2016) record of stream discharge from Leach et al. (2016) (Figure 7b). The total annual runoff across these different years varied from 240 to 834 mm and the total C export varied from 8 to 26 g C m<sup>-2</sup> yr<sup>-1</sup> (see Leach et al. (2016) for more information). This exercise allowed us to estimate that the  $^{14}\text{C}$  content of the total annual C export may increase by ca 2 %modern with nearly a tripling of the annual runoff (Figure 7b). Therefore, we conclude that the source of aquatic C export is relatively constant and resilient to changes in hydroclimatic conditions. Similar conclusions were reached by a recent study addressing potential influence of rising air temperatures (Wilson et al., 2016). The stability of the source of aquatic C export may persist given the forecasted hydroclimatic changes for the region (annual precipitation >17%, mean annual temperature >3.7°C, in the coming century) (Teutschbein, Grabs, Karlsen, Laudon, & Bishop, 2015).

The C cycling in northern peatlands is highly sensitive to a number of environmental changes, most of which are driven by climatic changes or anthropogenic disturbances. The flux components of the NECB are recognized to be influenced by changes in temperature (Dinsmore et al., 2013; Peichl et al., 2014; Wilson et al., 2016; Wu & Roulet, 2014), precipitation and cloud cover (Dinsmore et al., 2013; Nijp et al., 2015), timing and magnitude of the spring freshet (Ågren et al., 2008; Dyson et al., 2011), atmospheric  $\text{CO}_2$  increase (Freeman et al., 2004) or changes in vascular plant communities (Lafleur, Roulet, Bubier, Frolking, & Moore, 2003; Lund et al., 2010), sulfur and nitrogen deposition (Eriksson, Öquist, & Nilsson, 2010), and peatland management (Jauhainen, Limin, Silvennoinen, & Vasander, 2008; Waddington & Price, 2000). Here, we demonstrated that the source of aquatic C export from this boreal poor fen remains relatively unchanged despite large annual hydroclimatic variation. In addition, the aquatic C export was only to a small degree sustained by degradation of ancient peat C stocks and was instead mainly supported by young C sources. It is worth noting that a growing body of evidence demonstrates the highly sensitive nature of peat C stock mobility to anthropogenic disturbances (Butman et al., 2014; Evans et al., 2014; Moore et al., 2013), an aspect that is not significant for this pristine boreal fen. Some of the  $^{14}\text{C}$  patterns reported here have seldom been documented in previous studies and appear to differ noticeably from the existing literature. Further  $^{14}\text{C}$  characterization of dissolved and gaseous C at other sites will be necessary to determine whether Degerö is unique in terms of C sources and transport dynamics, and to more completely assess the overall stability of

northern peatland C stocks. It is however, noteworthy that a boreal peatland that has been accumulating organic C since ~8,000 BP currently appears resilient, showing little or no evidence of ancient C release into the aquatic environment.

## ACKNOWLEDGEMENTS

This study was supported by the Swedish Research Council (contract: 2012–3919 to K. Bishop), the department of Earth Sciences at Uppsala University and the Knut and Alice Wallenberg foundation for financial support. This work was also supported by the Natural Environment Research Council (NERC) Radiocarbon Facility NRCF010001 (allocation number 15.1104 and 1947.1015). We thank the crew of the Krycklan Catchment Study (KCS) for great field support as well as the Swedish University of Agricultural Sciences Department of Aquatic Sciences and Assessment for laboratory analysis

## REFERENCES

- Åberg, J., & Wallin, M. B. (2014). Evaluating a fast headspace method for measuring DIC and subsequent calculation of  $p\text{CO}_2$  in freshwater systems. *Inland Waters*, 4, 157–166.
- Ågren, A., Berggren, M., Laudon, H., & Jansson, M. (2008). Terrestrial export of highly bioavailable carbon from small boreal catchments in spring floods. *Freshwater Biology*, 53, 964–972.
- Aravena, R., Warner, B., Charman, D., Belyea, L., Mathur, S., & Dinel, H. (1993). Carbon isotopic composition of deep carbon gases in an ombrogenous peatland, northwestern Ontario, Canada. *Radiocarbon*, 35, 271–276.
- Bellisario, L. M., Bubier, J. L., Moore, T. R., & Chanton, J. P. (1999). Controls on  $\text{CH}_4$  emissions from a northern peatland. *Global Biogeochemical Cycles*, 13, 81–91.
- Billett, M. F., Garnett, M. H., & Dinsmore, K. J. (2015). Should aquatic  $\text{CO}_2$  evasion be included in contemporary carbon budgets for peatland ecosystems? *Ecosystems*, 18, 471–480.
- Billett, M. F., Garnett, M. H., Dinsmore, K. J., Dyson, K. E., Harvey, F., Thomson, A. M., ... Kortelainen, P. (2012). Age and source of different forms of carbon released from boreal peatland streams during spring snowmelt in E. Finland. *Biogeochemistry*, 111, 273–286.
- Billett, M. F., Garnett, M. H., & Harvey, F. (2007). UK peatland streams release old carbon dioxide to the atmosphere and young dissolved organic carbon to rivers. *Geophysical Research Letters*, 34, L23401 <https://doi.org/10.1029/2007GL031797>.
- Butman, D. E., Wilson, H. F., Barnes, R. T., Xenopoulos, M. A., & Raymond, P. A. (2014). Increased mobilization of aged carbon to rivers by human disturbance. *Nature Geoscience*, 8, 112–116.
- Chanton, J. P., Bauer, J. E., Glaser, P. A., Siegel, D. I., Kelley, C. A., Tyler, S. C., ... Lazrus, A. (1995). Radiocarbon evidence for the substrates supporting methane formation within northern Minnesota peatlands. *Geochimica et Cosmochimica Acta*, 59, 3663–3668.
- Chanton, J. P., Glaser, P. H., Chasar, L. S., Burdige, D. J., Hines, M. E., Siegel, D. I., ... Cooper, W. T. (2008). Radiocarbon evidence for the importance of surface vegetation on fermentation and methanogenesis in contrasting types of boreal peatlands. *Global Biogeochemical Cycles*, 22, GB4022 <https://doi.org/10.1029/2008GB003274>.
- Charman, D. J., Aravena, R., Bryant, C. L., & Harkness, D. D. (1999). Carbon isotopes in peat, DOC,  $\text{CO}_2$ , and  $\text{CH}_4$  in a Holocene peatland on Dartmoor, southwest England. *Geology*, 27, 539–542.
- Chasar, L. S., Chanton, J. P., Glaser, P. H., Siegel, D. I., & Rivers, J. S. (2000). Radiocarbon and stable carbon isotopic evidence for transport

- and transformation of dissolved organic carbon, dissolved inorganic carbon, and CH<sub>4</sub> in a northern Minnesota peatland. *Global Biogeochemical Cycles*, 14, 1095–1108.
- Clymo, R. S., & Bryant, C. L. (2008). Diffusion and mass flow of dissolved carbon dioxide, methane, and dissolved organic carbon in a 7-m deep raised peat bog. *Geochimica et Cosmochimica Acta*, 72, 2048–2066.
- Corbett, E. J., Burdige, D. J., Tfaily, M. M., Dial, A. R., Cooper, W. T., Glaser, P. H., & Chanton, J. P. (2013). Surface production fuels deep heterotrophic respiration in northern peatlands. *Global Biogeochemical Cycles*, 27, 1163–1174.
- Crowther, T. W., Todd-Brown, K. E. O., Rowe, C. W., Wieder, W. R., Carey, J. C., Machmuller, M. B., ... Bradford, M. A. (2016). Quantifying global soil carbon losses in response to warming. *Nature*, 540, 104–108.
- Dinsmore, K. J., Billett, M. F., & Dyson, K. E. (2013). Temperature and precipitation drive temporal variability in aquatic carbon and GHG concentrations and fluxes in a peatland catchment. *Global Change Biology*, 19, 2133–2148.
- Dinsmore, K. J., Billett, M. F., Skiba, U. M., Rees, R. M., Drewer, J., & Helfter, C. (2010). Role of the aquatic pathway in the carbon and greenhouse gas budgets of a peatland catchment. *Global Change Biology*, 16, 2750–2762.
- Dyson, K., Billett, M., Dinsmore, K., Harvey, F., Thomson, A., Piirainen, S., & Kortelainen, P. (2011). Release of aquatic carbon from two peatland catchments in E. Finland during the spring snowmelt period. *Biogeochemistry*, 103, 125–142.
- Eriksson, T., Öquist, M. G., & Nilsson, M. B. (2010). Production and oxidation of methane in a boreal mire after a decade of increased temperature and nitrogen and sulfur deposition. *Global Change Biology*, 16, 2130–2144.
- Evans, C. D., Page, S. E., Jones, T., Moore, S., Gauci, V., Laiho, R., ... Garnett, M. H. (2014). Contrasting vulnerability of drained tropical and high-latitude peatlands to fluvial loss of stored carbon. *Global Biogeochemical Cycles*, 28, 1215–1234.
- Flury, S., Glud, R. N., Premke, K., & McGinnis, D. F. (2015). Effect of sediment gas voids and ebullition on benthic solute exchange. *Environmental Science & Technology*, 49, 10413–10420.
- Freeman, C., Fenner, N., Ostle, N. J., Kang, H., Dowrick, D. J., Reynolds, B., ... Hudson, J. (2004). Export of dissolved organic carbon from peatlands under elevated carbon dioxide levels. *Nature*, 430, 195–198.
- Frolking, S., Roulet, N. T., Moore, T. R., Richard, P. J. H., Lavoie, M., & Muller, S. D. (2001). Modeling northern peatland decomposition and peat accumulation. *Ecosystems*, 4, 479–498.
- Garnett, M. H., Billett, M. F., Gulliver, P., & Dean, J. F. (2016). A new field approach for the collection of samples for aquatic <sup>14</sup>C<sub>2</sub> analysis using headspace equilibration and molecular sieve traps: The super headspace method. *Ecology*, 9, 1630–1638.
- Garnett, M. H., Dinsmore, K. J., & Billett, M. F. (2012). Annual variability in the radiocarbon age and source of dissolved CO<sub>2</sub> in a peatland stream. *Science of The Total Environment*, 427–428, 277–285.
- Garnett, M. H., Gulliver, P., & Billett, M. F. (2016). A rapid method to collect methane from peatland streams for radiocarbon analysis. *Ecology*, 9, 113–121.
- Garnett, M., Hardie, S., & Murray, C. (2011). Radiocarbon and stable carbon analysis of dissolved methane and carbon dioxide from the profile of a raised peat bog. *Radiocarbon*, 53, 71–83.
- Garnett, M. H., Hardie, S. M. L., Murray, C., & Billett, M. F. (2013). Radiocarbon dating of methane and carbon dioxide evaded from a temperate peatland stream. *Biogeochemistry*, 114, 213–223.
- Garnett, M. H., Hartley, I. P., Hopkins, D. W., Sommerkorn, M., & Wooley, P. A. (2009). A passive sampling method for radiocarbon analysis of soil respiration using molecular sieve. *Soil Biology and Biochemistry*, 41, 1450–1456.
- Glaser, P. H., Siegel, D. I., Chanton, J. P., Reeve, A. S., Rosenberry, D. O., Corbett, J. E., ... Levy, Z. (2016). Climatic drivers for multidecadal shifts in solute transport and methane production zones within a large peat basin. *Global Biogeochemical Cycles*, 30, 1578–1598.
- Gorham, E. (1991). Northern peatlands: Role in the carbon cycle and probable responses to climatic warming. *Ecological Applications*, 1, 182–195.
- Granberg, G., Ottosson-Löfvenius, M., Grip, H., Sundh, I., & Nilsson, M. (2001). Effect of climatic variability from 1980 to 1997 on simulated methane emission from a boreal mixed mire in northern Sweden. *Global Biogeochemical Cycles*, 15, 977–991.
- Gut, A., Blatter, A., Fahrni, M., Lehmann, B. E., Neftel, A., & Staffelbach, T. (1998). A new membrane tube technique (METT) for continuous gas measurements in soils. *Plant and Soil*, 198, 79–88.
- Holden, J., & Burt, T. P. (2003). Runoff production in blanket peat covered catchments. *Water Resources Research*, 39, 1191.
- Holmes, M. E., Chanton, J. P., Tfaily, M. M., & Ogram, A. (2015). CO<sub>2</sub> and CH<sub>4</sub> isotope compositions and production pathways in a tropical peatland. *Global Biogeochemical Cycles*, 29, 1–18.
- Hornibrook, E. R. C., Longstaffe, F. J., & Fyfe, W. S. (2000). Evolution of stable carbon isotope compositions for methane and carbon dioxide in freshwater wetlands and other anaerobic environments. *Geochimica et Cosmochimica Acta*, 64, 1013–1027.
- Ingram, H. A. P. (1982). Size and shape in raised mire ecosystems: A geophysical model. *Nature*, 297, 300–303.
- Jauhainen, J., Limin, S., Silvennoinen, H., & Vasander, H. (2008). Carbon dioxide and methane fluxes in drained tropical peat before and after hydrological restoration. *Ecology*, 89, 3503–3514.
- Johnson, M. S., Billett, M. F., Dinsmore, K. J., Wallin, M., Dyson, K. E., & Jassal, R. S. (2010). Direct and continuous measurement of dissolved carbon dioxide in freshwater aquatic systems—method and applications. *Ecology*, 3, 68–78.
- Kotsyurbenko, O. R., Chin, K.-J., Glagolev, M. V., Stubner, S., Simankova, M. V., Nozhevnikova, A. N., & Conrad, R. (2004). Acetoclastic and hydrogenotrophic methane production and methanogenic populations in an acidic West-Siberian peat bog. *Environmental Microbiology*, 6, 1159–1173.
- Lafleur, P. M., Roulet, N. T., Bubier, J. L., Frolking, S., & Moore, T. R. (2003). Interannual variability in the peatland-atmosphere carbon dioxide exchange at an ombrotrophic bog. *Global Biogeochemical Cycles*, 17, 1036.
- Larsson, A., Segerström, U., Laudon, H., & Nilsson, M. B. (2016). Holocene carbon and nitrogen accumulation rates in a boreal oligotrophic fen. *The Holocene*, 27(6), 811–821.
- Laudon, H., Berggren, M., Ågren, A., Buffam, I., Bishop, K., Grabs, T., ... Köhler, S. (2011). Patterns and dynamics of dissolved organic carbon (DOC) in boreal streams: The role of processes, connectivity, and scaling. *Ecosystems*, 14, 880–893.
- Laudon, H., Sjöblom, V., Buffam, I., Seibert, J., & Morth, M. (2007). The role of catchment scale and landscape characteristics for runoff generation of boreal streams. *Journal of Hydrology*, 344, 198–209.
- Laudon, H., Taberman, I., Ågren, A., Futter, M., Ottosson-Löfvenius, M., & Bishop, K. (2013). The Krycklan Catchment Study—A flagship infrastructure for hydrology, biogeochemistry, and climate research in the boreal landscape. *Water Resources Research*, 49, 7154–7158.
- Leach, J. A., Larsson, A., Wallin, M. B., Nilsson, M. B., & Laudon, H. (2016). Twelve year interannual and seasonal variability of stream carbon export from a boreal peatland catchment. *Journal of Geophysical Research: Biogeosciences*, 121, 1851–1866.
- Leith, F. I., Garnett, M. H., Dinsmore, K. J., Billett, M. F., & Heal, K. V. (2014). Source and age of dissolved and gaseous carbon in a peatland-riparian-stream continuum: A dual isotope (<sup>14</sup>C and <sup>δ</sup><sup>13</sup>C) analysis. *Biogeochemistry*, 119, 415–433.
- Levin, I., Hammer, S., Kromer, B., & Meinhardt, F. (2008). Radiocarbon observations in atmospheric CO<sub>2</sub>: Determining fossil fuel CO<sub>2</sub> over

- Europe using Jungfraujoch observations as background. *Science of The Total Environment*, 391, 211–216.
- Lund, M., Lafleur, P. M., Roulet, N. T., Lindroth, A., Christensen, T. R., Aurela, M., ... Nilsson, M. B. (2010). Variability in exchange of CO<sub>2</sub> across 12 northern peatland and tundra sites. *Global Change Biology*, 16, 2436–2448.
- Marwick, T. R., Tamooh, F., Teodoru, C. R., Borges, A. V., Darchambeau, F., & Bouillon, S. (2015). The age of river-transported carbon: A global perspective. *Global Biogeochemical Cycles*, 29, 122–137.
- Mayorga, E., Aufdenkampe, A. K., Masiello, C. A., Krusche, A. V., Hedges, J. I., Quay, P. D., ... Brown, T. A. (2005). Young organic matter as a source of carbon dioxide outgassing from Amazonian rivers. *Nature*, 436, 538–541.
- Mccallister, S. L., & Del Giorgio, P. A. (2012). Evidence for the respiration of ancient terrestrial organic C in northern temperate lakes and streams. *Proceedings of the National Academy of Sciences*, 109, 16963–16968.
- Moore, S., Evans, C. D., Page, S. E., Garnett, M. H., Jones, T. G., Freeman, C., ... Gauci, V. (2013). Deep instability of deforested tropical peatlands revealed by fluvial organic carbon fluxes. *Nature*, 493, 660–663.
- Nijp, J. J., Limpens, J., Metselaar, K., Peichl, M., Nilsson, M. B., van der Zee, S. E., & Berendse, F. (2015). Rain events decrease boreal peatland net CO<sub>2</sub> uptake through reduced light availability. *Global Change Biology*, 21, 2309–2320.
- Nilsson, M., Klarqvist, M., Bohlin, E., & Possnert, G. (2001). Variation in <sup>14</sup>C age of macrofossils and different fractions of minute peat samples dated by AMS. *The Holocene*, 11, 579–586.
- Nilsson, M., Sagerfors, J., Buffam, I., Laudon, H., Eriksson, T., Grelle, A., ... Lindroth, A. (2008). Contemporary carbon accumulation in a boreal oligotrophic minerogenic mire – a significant sink after accounting for all C-fluxes. *Global Change Biology*, 14, 2317–2332.
- Öquist, M. G., Wallin, M., Seibert, J., Bishop, K., & Laudon, H. (2009). Dissolved inorganic carbon export across the soil/stream interface and its fate in a boreal headwater stream. *Environment Science and Technology*, 43, 7364–7369.
- Palmer, S., Hope, D., Billett, M., Dawson, J. C., & Bryant, C. (2001). Sources of organic and inorganic carbon in a headwater stream: Evidence from carbon isotope studies. *Biogeochemistry*, 52, 321–338.
- Peichl, M., Öquist, M., Ottosson, M., Ilstedt, U., Sagerfors, J., Grelle, A., ... Nilsson, M. B. (2014). A 12-year record reveals pre-growing season temperature and water table level threshold effects on the net carbon dioxide exchange in a boreal fen. *Environmental Research Letters*, 9, 055006.
- Peichl, M., Sagerfors, J., Lindroth, A., Buffam, I., Grelle, A., Klemedtsson, L., ... Nilsson, M. B. (2013). Energy exchange and water budget partitioning in a boreal minerogenic mire. *Journal of Geophysical Research: Biogeosciences*, 118, 1–13.
- Peralta-Tapia, A., Sponseller, R. A., Tetzlaff, D., Soulsby, C., & Laudon, H. (2015). Connecting precipitation inputs and soil flow pathways to stream water in contrasting boreal catchments. *Hydrological Processes*, 29, 3546–3555.
- R Core Team (2013). *R: A language and environment for statistical computing*. Vienna, Austria: R Foundation for Statistical Computing. Retrieved from <http://www.R-project.org/>.
- Ronkanen, A.-K., & Kløve, B. (2007). Use of stable isotopes and tracers to detect preferential flow patterns in a peatland treating municipal wastewater. *Journal of Hydrology*, 347, 418–429.
- Roulet, N. T., Lafleur, P. M., Richard, P. J., Moore, T. R., Humphreys, E. R., & Bubier, J. (2007). Contemporary carbon balance and late Holocene carbon accumulation in a northern peatland. *Global Change Biology*, 13, 397–411.
- Schiff, S., Aravena, R., Mewhinney, E., Elgood, R., Warner, B., Dillon, P., & Trumbore, S. (1998). Precambrian Shield wetlands: Hydrologic control of the sources and export of dissolved organic matter. *Climatic Change*, 40, 167–188.
- Schiff, S., Aravena, R., Trumbore, S. E., Hinton, M. J., Elgood, R., & Dillon, P. J. (1997). Export of DOC from forested catchments on the Precambrian Shield of Central Ontario: Clues from <sup>13</sup>C and <sup>14</sup>C. *Biogeochemistry*, 36, 43–65.
- Teutschbein, C., Grabs, T., Karlsen, R. H., Laudon, H., & Bishop, K. (2015). Hydrological response to changing climate conditions: Spatial stream-flow variability in the boreal region. *Water Resources Research*, 51, 9425–9446.
- Throckmorton, H. M., Heikoop, J. M., Newman, B. D., Altmann, G. L., Conrad, M. S., Muss, J. D., ... Wilson, C. J. (2015). Pathways and transformations of dissolved methane and dissolved inorganic carbon in Arctic tundra watersheds: Evidence from analysis of stable isotopes. *Global Biogeochemical Cycles*, 29, 1893–1910.
- Tipping, E., Billett, M. F., Bryant, C. L., Buckingham, S., & Thacker, S. A. (2010). Sources and ages of dissolved organic matter in peatland streams: Evidence from chemistry mixture modelling and radiocarbon data. *Biogeochemistry*, 100, 121–137.
- Vihermaa, L. E., Waldron, S., Garnett, M. H., & Newton, J. (2014). Old carbon contributes to aquatic emissions of carbon dioxide in the Amazon. *Biogeosciences Discussions*, 11, 1773–1800.
- Waddington, J., & Price, J. (2000). Effect of peatland drainage, harvesting, and restoration on atmospheric water and carbon exchange. *Physical Geography*, 21, 433–451.
- Wallin, M., Buffam, I., Öquist, M., Laudon, H., & Bishop, K. (2010). Temporal and spatial variability of dissolved inorganic carbon in a boreal stream network: Concentrations and downstream fluxes. *Journal of Geophysical Research: Biogeosciences*, 115, G02014 <https://doi.org/10.1029/2009JG001100>.
- Wallin, M. B., Grabs, T., Buffam, I., Laudon, H., Ågren, A., Öquist, M. G., & Bishop, K. (2013). Evasion of CO<sub>2</sub> from streams – The dominant component of the carbon export through the aquatic conduit in a boreal landscape. *Global Change Biology*, 19, 785–797.
- Whiticar, M. J., Faber, E., & Schoell, M. (1986). Biogenic methane formation in marine and freshwater environments: CO<sub>2</sub> reduction vs. acetate fermentation—Isotope evidence. *Geochimica et Cosmochimica Acta*, 50, 693–709.
- Wilson, R. M., Hopple, A. M., Tfaily, M. M., Sebestyen, S. D., Schadt, C. W., Pfeifer-Meister, L., ... Hanson, P. J. (2016). Stability of peatland carbon to rising temperatures. *Nature Communications*, 7, 13723.
- Winterdahl, M., Laudon, H., Lyon, S. W., Pers, C., & Bishop, K. (2016). Sensitivity of stream dissolved organic carbon to temperature and discharge: Implications of future climates. *Journal of Geophysical Research: Biogeosciences*, 121, 126–144.
- Wu, J., & Roulet, N. T. (2014). Climate change reduces the capacity of northern peatlands to absorb the atmospheric carbon dioxide: The different responses of bogs and fens. *Global Biogeochemical Cycles*, 28, 1005–1024.

## SUPPORTING INFORMATION

Additional Supporting Information may be found online in the supporting information tab for this article.

**How to cite this article:** Campeau A, Bishop KH, Billett MF, et al. Aquatic export of young dissolved and gaseous carbon from a pristine boreal fen: Implications for peat carbon stock stability. *Glob Change Biol*. 2017;23:5523–5536.

<https://doi.org/10.1111/gcb.13815>